PHYSICAL REVIEW D **75,** 054024 (2007)

Instantons, chiral dynamics, and hadronic resonances

M. Cristoforetti, P. Faccioli, and M. Traini

Dipartimento di Fisica and INFN, Università degli Studi di Trento, Via Sommarive 15, Povo, Trento 38050, Italy
and European Centre for Theoretical Studies in Nuclear Physics and Related Areas,
Strada delle Tabarelle 286, Villazzano, Trento, I-38050, Italy

(Received 2 February 2007; published 20 March 2007)

We use the interacting instanton liquid model (IILM) as a tool to study the role played by the chiral interactions in the lowest-lying vector and axial-vector meson resonances. We find that narrow a_1 and ρ meson resonances can be generated by instanton-induced chiral forces, even in the absence of confinement. In the IILM, these hadrons are found to have masses only about 30% larger than the experimental value and small width $\lesssim$ 10–50 MeV. This result suggests that chiral interactions are very important in these systems and provide most of their mass. We explore the decaying patterns of the ρ meson, in the absence of confinement. We argue that, in our model where only chiral forces are switched on, this meson decays dissociating into its quark-antiquark constituents.

DOI: 10.1103/PhysRevD.75.054024 PACS numbers: 12.38.−t, 11.15.Ex, 12.38.Gc, 12.40.−y

I. INTRODUCTION

Hadron spectroscopy provides basic constraints on the structure of nonperturbative QCD dynamics. Since gluons interact with quarks in a way which depends dramatically on the quark mass, we expect the light- and heavy-hadron sectors of the spectrum to be sensitive to different dynamical correlations. For example, while the charmonium spectrum is well understood in terms of a linearly rising confining potential and perturbative gluon exchange, the description of the light-hadron spectra in terms of QCD degrees of freedom must take into account also the interactions responsible for spontaneous breaking of chiral symmetry. In particular, we expect the mass and the structure of the lowest-lying hadrons such as pion, nucleon, vector, and axial-vector mesons to be strongly influenced by the chiral interactions, because the splitting between parity partners in this part of the spectrum is as large as 500–600 MeV. On the other hand, Regge trajectories suggest that resonances with large angular momentum are predominantly influenced by the physics of color confinement, and it has been conjectured that chiral symmetry breaking may be even restored up in the spectrum (see e.g. [1] and references therein). In this paper we address the following questions: are any of the light-hadron resonances generated predominantly by chiral forces, with confinement playing a subleading role? Could any of such hadrons exist even in the complete absence of confinement? In this case, would such systems still decay predominantly in colorless hadrons? What is the microscopic dynamical mechanism underlying the splitting between the different lowest-lying multiplets?

The answers to these questions root in the nonperturbative sector of QCD. Although lattice field theory provides the only available *ab initio* tool for computing nonperturbative QCD correlation functions, the mechanism by which the hadron structure arises is not directly evident in such a framework. In particular, it is difficult to disentangle the contribution to the correlation functions arising from the different types of interaction, such as the confining forces, the chiral forces, and the perturbative gluon exchange. Hence, in order to gain physics insight, in the present work we focus on the role played by chiral symmetry breaking and we do so by restricting the path integral to a sum over gauge field configurations which generate the near zero-mode zone of the Dirac operator. To this end, we adopt the interacting instanton liquid model, developed in [2]. Instantons have been long argued to be the dominant fluctuations generating the zero-mode zone of the Dirac operator, hence providing the correlations which break spontaneously chiral symmetry. In the IILM, the QCD path integral over all gluon configurations is replaced by an effective theory in which the gauge fields accounted for are those generated by integrating over the positions, color orientations, and sizes of singular-gauge instantons.

Several features of the instanton picture have been observed in a number of lattice studies [3–6]. In particular, it has been observed that chiral symmetry breaking in QCD is strongly correlated with smooth lumps of topological gauge fields, with a shape compatible with that of singular-gauge instantons [7,8].

Instanton-induced correlations in hadrons have also been studied through several phenomenological model calculations. It has been shown that instanton models provide a good description of the mass and the electroweak structure of pions, nucleons, and hyperons [9–18]. In a recent work [19], we have used the IILM to study the dependence of the Dirac spectrum and of the pion and nucleon masses on the current quark mass. We have found that the dependence of these observables on the pion mass is in quantitative agreement with both chiral perturbation theory and lattice simulations.

The main shortcoming of the instanton liquid model is that it does not lead to the correct behavior of the Wilson loop, i.e. it does not predict a linearly rising potential between static color sources, at large distances. This fact

implies that, while singular-gauge instantons accounts well for the nonperturbative QCD correlations at the chiral symmetry breaking scale $\Lambda_\chi \sim 1$ GeV, they do not generate sufficient long-range correlations at the confining scale $\sim\Lambda_{\rm QCD} \sim 0.2$ GeV. As a result, we expect the chiral forces generated by these topological fluctuations to play only a marginal role in heavy-quark systems—which are insensitive to chiral dynamics—or in highly excited hadrons—whose wave functions are expected to extend for several fm. On the other hand, just because of the lack of confinement, the IILM can be used as a tool to single out the contribution of chiral forces in the different hadronic systems. By studying where the model works well, we can identify the properties of the hadrons which are almost completely determined by the chiral dynamics. Conversely, by studying where the model fails, one can in principle gain information about the structure of the additional interaction which is needed in order to reproduce the experiment. In this context, a_1 and ρ resonances represent the ideal test systems: being in between the pion—which is strongly related to chiral symmetry breaking—and highly excited states—which are dominated by color confinement—they are expected to be sensitive to both chiral and confining interactions. In addition the splitting between these two resonance masses is a direct measure of the effect of spontaneous chiral symmetry breaking.

An exploratory study of the contribution of instanton forces to the lowest-lying hadrons was performed in [10,11], where several hadronic Euclidean point-to-point correlation functions were calculated in the IILM up to sizes of the order of several fractions of a fm. It was shown that instanton-induced chiral forces are very strongly attractive in the nucleon and pion, but much weaker in the ρ and Δ. Their study provides indications that hadron resonances might exist in the instanton vacuum. In fact ρ, a_1, and Δ masses extracted from a fit of the corresponding point-to-point correlation functions using a pole-plus-continuum ansatz for the spectral function, were found to be within 20%–30% from their experimental value.

In this model, the dynamical origin of the splitting between the hadron multiplets which are not connected via chiral transformations is well understood in terms of the diluteness of the instanton liquid. In fact, the instanton zero-mode contribution to the two-point correlation functions associated to the pion and to the nucleon comes at the lowest order in the instanton liquid diluteness $\kappa \sim 10^{-1}$. On the other hand, the analog contribution to the correlation functions associated to vector- and axial-vector mesons and to decuplet baryons masses comes at the next-to-leading order, i.e. to $\mathcal{O}(\kappa^2)$. The splitting between chiral partners is provided by the spontaneous chiral symmetry associated with the delocalization of the fermion zero-modes (see [20] and references therein).

In this context an interesting question is whether, in the presence of only instanton-induced chiral forces, the a_1 and ρ resonances predominantly tend to decay into colorless pions, or rather dissociate into free quarks and antiquarks. In the present work we address this and other related issues concerning the contribution of chiral dynamics to the structure of hadronic resonances by computing momentum projected correlation functions at Euclidean times up to $\sim$1.2 fm and we focus on the effective-mass plot.

This method is usually employed in lattice QCD simulations to extract the masses of the stable bound-states *only*, i.e. when the lowest-lying hadron contributes to the spectral density through a δ-function.

In this case, the effective-mass plot displays a flat plateau in the large Euclidean time limit. We extend this method to include the case in which the lowest-lying hadron is *not* a stable bound-state but rather a resonance with a finite width. In this case then effective-mass plot displays an approximately linear and mild falloff at intermediate Euclidean times. This behavior can be distinguished both from the flat plateau associated to stable bound-states and from the strong exponential decay associated to the filtering of a perturbative continuum. As a result both the mass and the width of the lowest-lying mesons and baryons can be extracted.

In addition, some information about the decay patterns of these resonances can be gained by studying the behavior of the effective mass in the asymptotically large Euclidean time. In this regime, the effective mass converges to the smallest eigenvalue in the transfer matrix. If the simulation box is sufficiently large, the lowest eigenvalue of the transfer matrix in the ρ and a_1 channels corresponds to the invariant mass of the branch-cut singularity in their two-point function. In QCD these are expected to be at the threshold for decaying into two and three pions, respectively. In models which do not account for confinement, these hadrons could also decay into free quarks and the branch-cut may be shifted.

We apply the effective-mass plot analysis to determine the mass of the lowest-lying vector and axial-vector meson, using several values of the quark mass. Our results clearly show that the instanton-induced chiral forces are sufficiently strong to generate the ρ meson and the a_1 meson resonances even in the absence of confinement.

On the other hand, while our previous studies have shown that the nucleon and pion masses are correctly reproduced in this model [19], the vector and axial-vector mesons resonances are found to be about 30% heavier than their experimental value, with $M_\rho \simeq 1$ GeV and $M_{a_1} \simeq 1.7$ GeV. These results support a picture in which the mass and binding of the nucleon and pion is almost entirely provided by chiral forces, while the mass of the vector and axial mesons receive a significant contribution from confinement interactions of the order of 30%.

For some of the quark masses we have used, the resulting mass of the ρ and a_1 resonances turn out to be sig-

nificantly smaller than the threshold for decaying into three and two pions, respectively. In the presence of confinement such hadrons would be stable. However, in our IILM calculations we find a ρ meson width of 10 MeV. Our interpretation of these results is that, in the presence of chiral interaction only, the ρ meson eventually tends to dissociate into its constituents.

In the next section we present our phenomenological approach to extract information about hadron resonances from the effective-mass plot. In Sec. III we present and discuss the results of our calculations. Section IV is devoted to the summary and conclusions.

II. RESONANCES AND THE EFFECTIVE-MASS PLOT

In QCD the information about the hadron spectrum is encoded in the two-point correlation functions, defined as

$$\Pi_H(\mathbf{x}, \tau) = \langle 0|T[J_H(\mathbf{x}, \tau)J_H^\dagger(\mathbf{0}, 0)]|0\rangle. \tag{1}$$

$J_H(\mathbf{x}, \tau)$ is an overlap operator that creates states with the quantum numbers of the hadron H. The lowest-dimensional overlap operators generating states with quantum numbers of π, ρ, a_1 mesons are:

$$J_H(x) = \bar{q}(x)\Gamma_H q(x), \tag{2}$$

$$\Gamma_\pi = \tau^+ i\gamma_5, \qquad \Gamma_\rho = \tau^+\gamma_\mu, \qquad \Gamma_{a_1} = \tau^+ i\gamma_5\gamma_\mu. \tag{3}$$

In the following we consider the effective mass $M_H^{\rm eff}(\tau)$, defined as

$$M_H^{\rm eff}(\tau) = \lim_{\Delta\tau\to 0}\frac{1}{\Delta\tau}\ln\left[\frac{G_H(\tau)}{G_H(\tau+\Delta\tau)}\right], \tag{4}$$

where $G_H(\tau)$ is the zero-momentum-projected hadronic two-point function,

$$G_H(\tau) = \int d^3\mathbf{x}\,\Pi_H(\mathbf{x}, \tau), \tag{5}$$

which can be written in the spectral representation:

$$G_H(\tau) = \int \frac{ds}{2\sqrt{s}}\rho_H(s)e^{-\sqrt{s}\tau}, \tag{6}$$

where $\rho_H(s)$ is the spectral function.

In the large Euclidean time limit, the effective mass filters out the lowest singularity in the two-point function, i.e. the smallest eigenvalue of the transfer matrix. If the lowest-lying state in a given channel is a stable hadron, then the two-point function develops a pole at the bound-state mass below the threshold of the branch-cut associated to multiparticle production. Then, the effective mass asymptotically approaches the value of the mass of the bound-state:

$$\lim_{\tau\to\infty} M_H^{\rm eff}(\tau) = M_H. \tag{7}$$

In QCD the only bound-states are pions and nucleons. In all the other channels, the two-point functions display branch-cut singularities only.

It is instructive to study the behavior of the effective-mass plot if the spectral function $\rho_H(s)$ displays a narrow resonance with a finite-width, emerging above a continuum background at small s and converging to the asymptotic perturbative continuum, in the large s limit. As a working example, we consider the effective-mass plot for the vector-meson channel. In this case, the spectral function can be extracted from the ALEPH Collaboration data [21] for τ decays in two pions. A reasonable parametrization of such data can be constructed from a Breit-Wigner function for the ρ meson resonance, supplemented by a term simulating the perturbative continuum (see Fig. 1, left panel) [22]:

$$\rho_\rho(s) = C_1^\rho\frac{(\Gamma_\rho/2)^2}{(\Gamma_\rho/2)^2 + (\sqrt{s} - m_\rho)^2} + \frac{C_2^\rho}{1 + \exp[(E_0 - \sqrt{s})/0.2]}. \tag{8}$$

The right panel shows the effective-mass plot obtained from a phenomenological parametrization of the two-point function, using Eqs. (4), (6), and (8). At small Euclidean times, $\tau \lesssim 0.4$ fm, the effective mass $M_{\rm eff}^H(\tau)$ drops exponentially. Such a rapid falloff is due to the exponential suppression of the perturbative continuum of excitations induced by the propagation in the imaginary time. At larger Euclidean times, $0.5\ {\rm fm} \lesssim \tau \lesssim 2$ fm, the effective mass displays a linear, nearly flat region. In this regime, the spectral representation of $M_{\rm eff}^H(\tau)$ is dominated by the ρ meson resonance peak. In fact, it is easy to check that, in the limit of vanishing width, one recovers a completely flat straight line, i.e. the familiar signature of a stable bound-state. Eventually, at even larger τ, the effective mass slowly converges to the threshold energy for multiparticle production.[1] We stress the fact that the effective-mass plot analysis is much more efficient than the corresponding point-to-point correlation function study in distinguishing a resonance peak from a stable bound-state.

From this discussion it follows that it is in principle possible to extract the width of the resonance from the effective-mass plot in the intermediate Euclidean time region. We note that, in (unquenched) lattice simulations, the stability of all hadrons except nucleon and pions depends on the size of the simulation box and on the value of the pion mass used. For example, at large pion masses $2m_\pi > m_\rho$ the ρ meson is a stable state, because there is no phase-space available for decaying into two pions. In

[1]Note that, since our simple phenomenological parametrization (8) does not vanish below the two-pion threshold, $s = \sqrt{2m_\pi}$, the resulting effective mass converges to 0 in the asymptotically large Euclidean times.

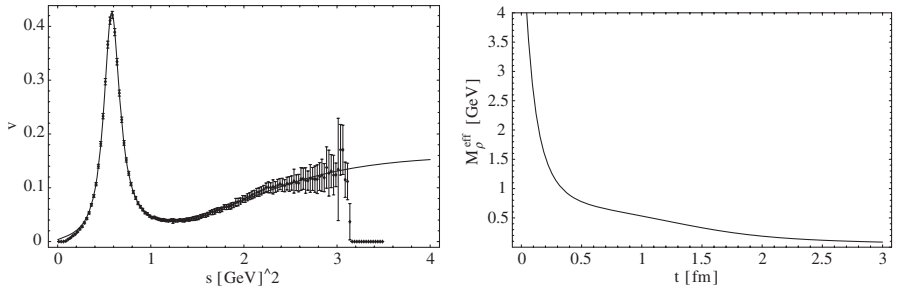

FIG. 1. Left panel: parametrization of the ALEPH Collaboration [21] data for the vector spectral density. Right panel: the corresponding effective-mass plot.

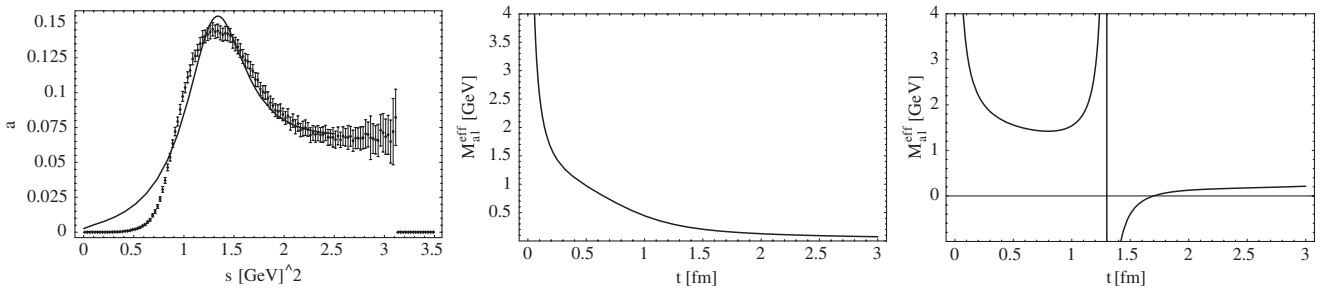

FIG. 2. Left panel: parametrization of the ALEPH Collaboration data [21] for τ decays in three pions using Eq. (9). Center panel: the corresponding phenomenological effective-mass plot for the a_1 meson. Right panel: effective-mass plot for the a_1 meson with reduced width $\Gamma_{a_1} = 0.03$ GeV.

this case, one can simply read off its mass from the plateau in the effective-mass plot, at large Euclidean times.

On the other hand, for sufficiently small pion masses, the phase-space for decaying into two pions opens up and the ρ meson appears in the spectral density as a resonance. In this case, the smallest eigenvalue of the transfer matrix filtered out by the propagation in imaginary time is related to the two-pion p-wave state. Note however that, if the periodic box is too small, the quantization of momentum may shift the p-wave two-pion state threshold above the ρ meson mass. As an example, let us consider a simulation performed in a box with size of $L = 2.5$ fm and with a pion mass of 500 MeV. In this case, the smallest nonvanishing unit of momentum is $2\pi/L \simeq 500$ MeV, and the threshold for decay into a two-pion p-wave state is at $2\sqrt{m_\pi^2 + (\pi/L)^2} \simeq 1.1$ GeV which can be above the ρ meson mass.

Note that in our IILM calculations we do not have to worry about effects related to quantization of momentum, as we do not adopt periodic boundary conditions. Instead, we choose simulation boxes which are sufficiently large for the integrand $\Pi_H(\mathbf{x}, \tau)$ in the momentum projection integral (5) to become very small and negligible near the borders of the box.[2] Under such conditions, the lowest point in the branch-cut for the ρ meson two-point correlation function is located at the threshold for two-pion production, i.e. $\sqrt{s} = 2M_\pi$.

Let us now discuss the axial-vector channel. In this case, the hadronic current has an overlap with both the pion state and the a_1 resonance. A rough parametrization of the ALEPH Collaboration data [21] for τ decays into three pions (see the left panel of Fig. 2) leads to the spectral function [22]:

$$\rho(s) = C_1^{a_1} \frac{(\Gamma_{a_1}/2)^2}{(\Gamma_{a_1}/2)^2 + (\sqrt{s} - m_{a_1})^2} - f_\pi^2 m_\pi^2 \delta(s - m_\pi^2) + \frac{C_2^{a_1}}{1 + \exp[(E_0 - \sqrt{s})/0.2]}, \quad (9)$$

where the pion pole arises from the matrix element $\langle 0|J_5^\mu(0)|\pi\rangle = ip_\mu f_\pi$. We note that the pion contribution to this spectral function comes with an opposite sign with respect to that of the a_1 resonance. Using (9) and dialing the physical value for m_π and f_π, we obtain the effective-mass plot shown in the central panel of Fig. 2. This plot displays a structure which is qualitatively similar to that of the vector-meson channel. On the other hand, dramatic differences emerge when the width of the a_1 is reduced (for instance because of heavy pions in the spectrum). For example, if we reduce Γ_{a_1} by 1 order of magnitude we obtain the effective-mass plot shown in the right panel of Fig. 2. In the limit of stable a_1 (vanishing width), a singu-

[2]Note that this is different from imposing Dirichlet boundary conditions, as we do not impose wave functions or correlators to vanish at the border of the box.

larity develops at the Euclidean time

$$\tau = \frac{1}{M_{a_1} - M_\pi} \log\left[\frac{\Lambda_{a_1}^2}{f_\pi^2 m_\pi^2}\right], \tag{10}$$

where Λ_{a_1} is the coupling of the axial-vector current to the a_1 state. This is a consequence of the cancellation between the contributions of the pion and axial-vector poles in the denominator of Eq. (4).

In the next section we compare these phenomenological representations of the effective-mass plot with the results of calculations performed in the IILM.

III. RESULTS AND DISCUSSION

In the IILM, hadronic correlation functions are evaluated by means of Monte Carlo averages over instanton ensemble configurations. The only phenomenological parameters of the model are the instanton average size $\bar{\rho} = 0.33$ fm and the dimensionless strength of the instanton-anti-instanton bosonic short-distance repulsion (for a concise review of this model see [19], for an extended treatment see [20]). In the present calculations we used five sets of ensemble configurations, corresponding to quark masses ranging from 20 to 90 MeV and we estimated statistical errors using jackknife technique, with bin size of 10 configurations. In order to isolate the instanton-induced chiral interactions, we have adopted the so-called zero-mode approximation, in which the part of the quark propagator which does not receive contribution from the instanton zero-modes has been replaced by a free propagator (for further details, see the discussions in [19,20]). For comparison, we have performed the same calculations also including the nonzero-mode part of the propagator and we have not found significant differences, hence instanton-induced correlations not associated to the chiral zero-mode zone play only a marginal role.

Our results for the calculation of the ρ meson effective mass for several quark masses are shown in Fig. 3, where they are compared with the best fit obtained from the phenomenological representation of the spectral function (8). The IILM points can be very well interpolated throughout the entire region 0.4 fm $\lesssim \tau \lesssim$ 1.2 fm. On the other

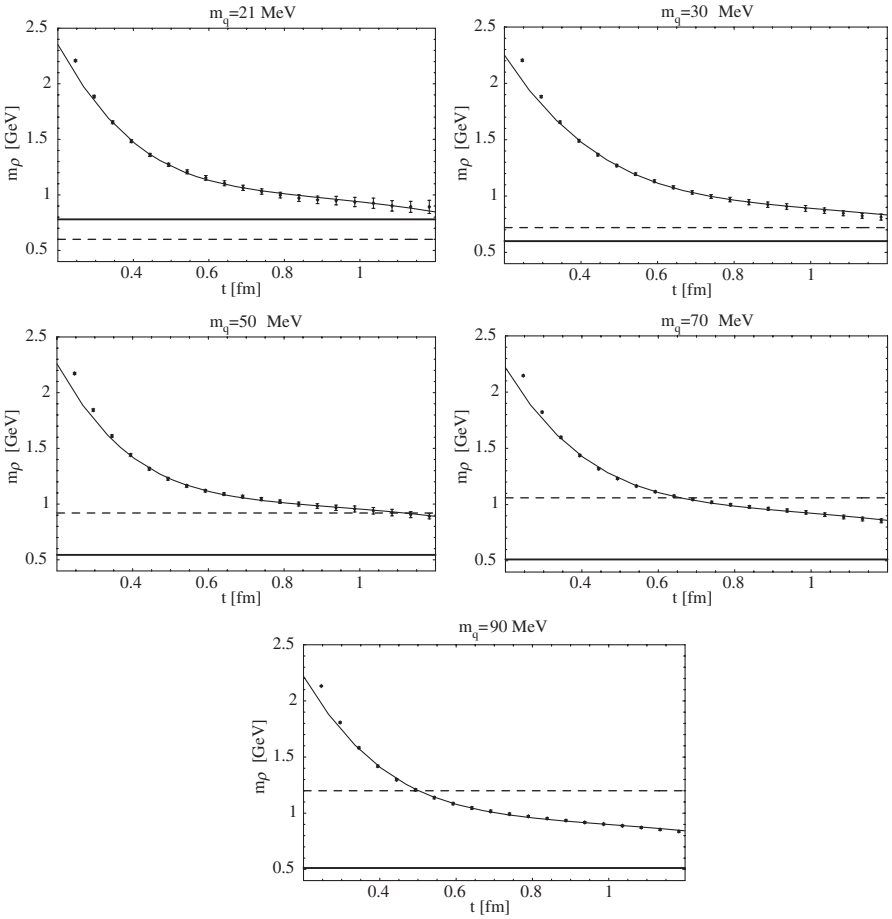

FIG. 3. Effective-mass plots in the ρ meson channel evaluated in the IILM at different quark masses and compared to the phenomenological parametrization (solid line). The dashed straight line represents the expected asymptotic plateau if the ρ meson decays into two pions, while the solid straight line represents the expected asymptotic plateau if the ρ meson decays into two constituent quarks with masses estimated from the IILM calculation in [24].

hand, it should be noted that a fit of these points using a spectral function which does not account for a narrow meson resonance would be inconsistent with our IILM points. The ρ meson contribution is needed to explain the nearly flat behavior of the effective mass for $\tau >$ 0.6 fm.

Our results for the calculation of the a_1 meson effective mass for several quark masses are shown in Fig. 4, where they are compared with the best fit obtained from the phenomenological representation of the spectral function (9). In order to reduce the number of free fitting parameters, we have chosen to neglect the contribution of the continuum, and to restrict the fit of the IILM points to the region $\tau > 0.6$ fm. In addition, we have used the value for the pion mass and decay constant calculated in the IILM in [19]. The qualitative behavior predicted in the previous section is very well reproduced by our model. In particular, we observe that the singularity arising from the cancellation of the π and a_1 contribution to the two-point correlator is clearly developed. This result provides a clean evidence that both the pion and the a_1 meson exist in the instanton vacuum. We note that, in this channel, the simple parametrization (9) of the ALEPH Collaboration data [21] is quite poor in the low s region. This is presumably the source of the small discrepancy observed for some quark masses, at the largest Euclidean times.

TABLE I. π, ρ, a_1 masses (in GeV units) calculated in the IILM for different quark masses.

m_q	M_π	M_ρ	M_{a_1}	Γ_ρ	Γ_{a_1}
0.02	0.30 ± 0.04	1.0 ± 0.1	1.6 ± 0.1	$\simeq 0.01$	<0.02
0.03	0.36 ± 0.04	0.9 ± 0.1	1.6 ± 0.1	$\lesssim 0.01$	<0.03
0.05	0.46 ± 0.04	1.0 ± 0.1	1.7 ± 0.1	$\simeq 0.05$	<0.01
0.07	0.53 ± 0.04	1.0 ± 0.1	1.7 ± 0.1	$\simeq 0.05$	<0.01
0.09	0.60 ± 0.04	0.9 ± 0.1	1.8 ± 0.2	$\simeq 0.05$	<0.01

For comparison, in Fig. 5 we show our effective-mass plots for the pion, which were obtained in [19] and display a completely flat behavior at large Euclidean times.

The complete list of ρ meson and a_1 masses extracted from the fit of the effective-mass plot are summarized in Table I. In general the masses obtained in the IILM are about 30% larger than the corresponding experimental

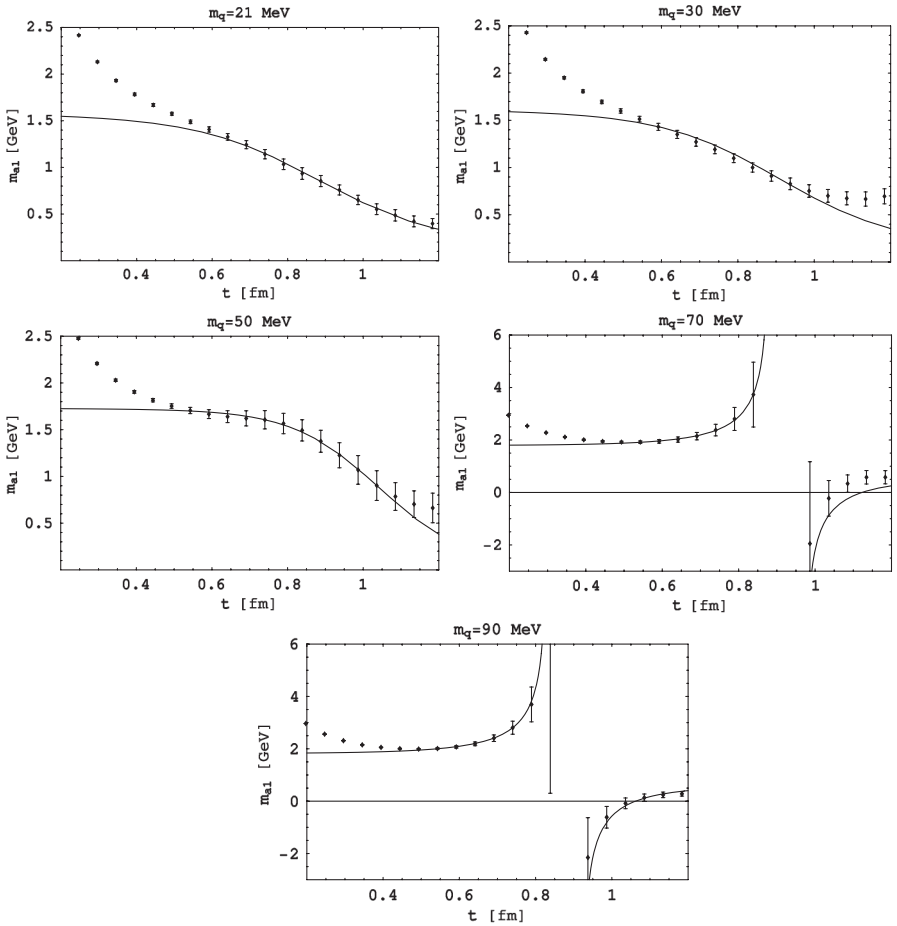

FIG. 4. Effective-mass plots in the a_1 meson channel, evaluated in the IILM at different quark masses and compared to the phenomenological parametrization (solid line). The latter does not include the contribution from the perturbative continuum (see discussion in the text).

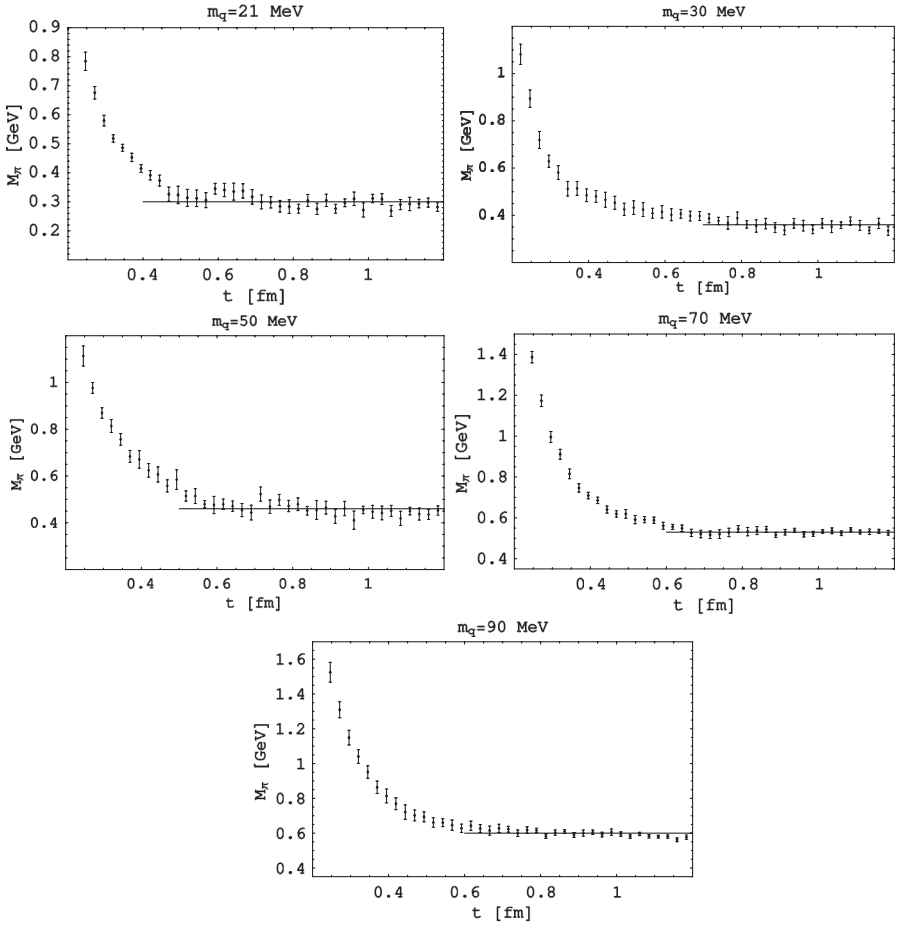

FIG. 5. Effective-mass plots for the pion evaluated in the IILM in [19].

values. This discrepancy suggests that about $1/4$ of the resonance mass is due to correlations which are not related to chiral symmetry breaking. This hypothesis is confirmed by the fact that the chiral asymmetry,

$$\chi = \frac{m_{a_1} - m_\rho}{m_{a_1} + m_\rho}, \tag{11}$$

which has been suggested as a parameter quantifying the contribution of chiral forces to hadron mass splittings [23], is remarkably well reproduced in this model. At the lightest quark mass we find $\chi^{\mathrm{IILM}} \simeq 0.2$, which should be confronted with the experimental value $\chi^{\mathrm{exp}} = 0.23$.

Let us now look in more detail on the mechanism of meson decay and we focus on the ρ meson in the IILM. The effective-mass plots in the vector-meson channel calculated at different quark masses are consistent with a small width spanning from 10 MeV to 50 MeV. Interestingly, the vector meson is always unstable in this model, even at quark masses for which there is no phase-space for decaying into pions, since $2M_\pi > M_\rho$. A natural explanation of this fact is that, in the absence of confinement, these hadrons decay into their quark-antiquark constituents. In the instanton vacuum, quarks acquire an effective mass as a consequence of the spontaneous breaking of chiral symmetry. Such a ''constituent'' quark mass at rest M_q was calculated in several approaches and found to range from $\simeq 400$ MeV to 200 MeV, depending on the bare quark mass (see e.g. [24] and references therein). In Fig. 3, we compare the effective-mass plot for the ρ meson with the $2M_\pi$ line, and the $2M_q$ line calculated in our model. We can see that, for the two largest quark masses, the effective mass falls below the $2M_\pi$ line, but always remains above the $2M_q$ line. Hence, there is always phase-space available to decay into constituent quarks.

IV. CONCLUSIONS

In this work we have studied the contribution of instanton-induced chiral forces in the a_1 and ρ meson resonances.

We have provided clean evidence that the a_1 and ρ meson can exist even in the presence of instanton forces only (i.e. in the instanton vacuum). Their masses extracted from a fit of the effective-mass plot have been found to be about 30% larger than the corresponding experimental values. This deviation should be confronted with the excellent agreement with the experimental masses previously found in the case of the pion and the nucleon [19]. These

results suggest that chiral forces are weaker in these resonances, but still represent the leading source of interactions.

On the other hand, the confining forces are very important to determine the width of these resonances and their decay properties. In fact, we have observed that, in this model, the vector meson is unstable even when quark masses are large and there is no phase-space to decay into two pions. This can be explained assuming that—as a consequence of the absence of confinement—mesons can dissociate into their constituents.

In the future, it would be interesting to study how the stability of the meson is restored, once confinement is introduced in the model. A way to do so would be to extend the ensemble of gauge configurations to include regular-gauge instantons and to study the behavior of the effective mass as a function of the density of such pseudoparticles [25].

ACKNOWLEDGMENTS

We thank John W. Negele for help and illuminating discussions. This work was supported in part by the U.S. DOE office of Nuclear Physics under Contract No. FC02-94ER40818 and the INFN-MIT ''Bruno Rossi'' Exchange Program.

[1] L. Y. Glozman, hep-ph/0609230.
[2] T. Schaefer and E. Shuryak, Phys. Rev. D **53**, 6522 (1996).
[3] M. Chu, J. Grandy, S. Huang, and J. W. Negele, Phys. Rev. D **49**, 6039 (1994).
[4] T. A. DeGrand and A. Hasenfratz, Phys. Rev. D **64**, 034512 (2001).
[5] P. Faccioli and T. A. DeGrand, Phys. Rev. Lett. **91**, 182001 (2003).
[6] P. Boucaud *et al.*, J. High Energy Phys. 04 (2003) 005.
[7] C. Gattringer, M. Gockeler, P. Rakow, S. Schaefer, and A. Schafer, Nucl. Phys. **B617**, 101 (2001).
[8] C. Gattringer, Phys. Rev. Lett. **88**, 221601 (2002).
[9] P. Faccioli, Int. J. Mod. Phys. A **20**, 4615 (2005).
[10] E. Shuryak and J. Verbaarschot, Nucl. Phys. **B410**, 55 (1993).
[11] E. Shuryak and J. Verbaarschot, Nucl. Phys. **B412**, 143 (1994).
[12] P. Faccioli and E. Shuryak, Phys. Rev. D **65**, 076002 (2002).
[13] P. Faccioli, A. Schwenk, and E. Shuryak, Phys. Lett. B **549**, 93 (2002).
[14] P. Faccioli, Phys. Rev. C **69**, 065211 (2004).
[15] P. Faccioli, A. Schwenk, and E. Shuryak, Phys. Rev. D **67**, 113009 (2003).
[16] M. Cristoforetti, P. Faccioli, E. Shuryak, and M. Traini, Phys. Rev. D **70**, 054016 (2004).
[17] M. Cristoforetti, P. Faccioli, G. Ripka, and M. Traini, Phys. Rev. D **71**, 114010 (2005).
[18] D. Diakonov, hep-ph/9602375.
[19] M. Cristoforetti, P. Faccioli, M. Traini, and J. Negele, Phys. Rev. D **75**, 034008 (2007).
[20] T. Schaefer and E. Shuryak, Rev. Mod. Phys. **70**, 323 (1998).
[21] R. Barate *et al.* (ALEPH Collaboration), Eur. Phys. J. C **4**, 409 (1998).
[22] E. Shuryak, Rev. Mod. Phys. **65**, 1 (1993).
[23] L. Y. Glozman, Acta Phys. Pol. B **35**, 2985 (2004).
[24] M. Musakhanov, in *Hadrons and Nuclei*, AIP Conf. Proc. No. 594 (AIP, New York, 2001), p. 357.
[25] J. Negele, F. Lenz, and M. Thies, Nucl. Phys. B, Proc. Suppl. **140**, 629 (2005).